JOURNAL OF AGRICULTURAL AND FOOD CHEMISTRY

Article

pubs.acs.org/JAFC

Comparison of Inhibitory Activities and Mechanisms of Five Mulberry Plant Bioactive Components against α-Glucosidase

Hao He[†] and Yan-Hua Lu*[,†]

[†]State Key Laboratory of Bioreactor Engineering, East China University of Science and Technology, Shanghai, P. R. China

Supporting Information

ABSTRACT: The α-glucosidase inhibitory effects of five bioactive components, namely 1-deoxynojirimycin, cyanidin-3-glucoside, cyanidin-3-rutinoside, resveratrol and oxyresveratrol contained in mulberry (*Morus, Moraceae*) plants have been compared. Spectroscopy methods were employed to compare their α-glucosidase inhibitory mechanisms. The results revealed that 1-deoxynojirimycin (competitive), resveratrol and oxyresveratrol (noncompetitive) were stronger inhibitors than acarbose, while cyanidin-3-glucoside and cyanidin-3-rutinoside (mix competitive and noncompetitive) showed modest activities. 1-Deoxynojirimycin, resveratrol and oxyresveratrol could quench the fluorescence spectra statically by forming stable complexes, while the quenching of cyanidin-3-rutinoside and cyanidin-3-glucoside belonged to dynamic quenching by the collision of molecules. The interactions between ligands and α-glucosidase were mainly driven by hydrophobic force, or hydrogen bonding consequently induced conformational changes and reduced surface hydrophobicity. Docking results suggested that they could bind to α-glucosidase at different sites. This work provides useful information for the understanding of the ligands−α-glucosidase interactions and identifies oxyresveratrol as a potent α-glucosidase inhibitor.

KEYWORDS: *α-glucosidase, 1-deoxynojirimycin, resveratrol, oxyresveratrol, cyanidin-3-glucoside, cyanidin-3-rutinoside, interaction*

INTRODUCTION

Elevated postprandial glucose which is one of the earliest abnormalities of glucose homeostasis associated with diabetes will increase the risk of developing microvascular complications and cardiovascular disease. Therapies focusing on achieving normal glycemia are effective in improving postprandial glycemic control and delaying the progression of long-term diabetic complications.[1,2] Thus, much attention has been drawn to gastrointestinal hydrolases particularly α-glucosidase which plays a central role in glycemic control. The clinically used α-glucosidase inhibitors, including acarbose,[3] miglitol and voglibose,[4] can bind to the α-glucosidase and competitively inhibit the enzyme in the small intestine to delay the expeditious generation of blood glucose. Unfortunately, these drugs often showed some adverse effects such as flatulence and diarrhea and might induce hepatotoxicity in chronic therapy.[3−5] Recent warnings about side effects of antidiabetic drugs highlight the urgent need of alternative and safer treatments, ideally through dietary polyphenols or a new type of drug.

Mulberry (*Morus, Moraceae*) plants are distributed widely in China. Both fruits and leaves from *Morus* have been used as medicinal materials and nutritional foodstuff.[6] Mulberry leaf can significantly reduce postprandial hyperglycemia in diabetic and healthy animals and exhibit fewer adverse side effects than other α-glucosidase inhibitors.[7,8] It is reported that 1-deoxynojirimycin (DNJ, Figure 1), a main alkaloid component in mulberry leaf, is the main hypoglycemic ingredients of mulberry leaf.[9−11] It can suppress different sources of α-glucosidase in a competitive manner, for example, rat intestinal, human lysosomal and yeast.[12,13] Otherwise, mulberry leaves also contain oxyresveratrol (OXY, Figure 1), which is only found in a limited number of plants. Although there is no study focused on hypoglycemic effects of OXY, it may also be a potent glucosidase inhibitor since it is a structural analogue of resveratrol (RES, Figure 1) which has been reported to have significant hypoglycemic activity.[14,15] Moreover, Mulberry fruit potentially exhibits a hypoglycemic effect and contains many bioactive components including cyanidin-3-glucoside (C3G), cyanidin-3-rutinoside (C3R) and RES.[16] It suggested that C3G and C3R (Figure 1) could suppress intestinal sucrase effectively and had synergistic effects with acarbose.[17,18] RES has received much attention based on its potential anticancer, neuroprotectant, cardioprotective and antidiabetic effects. The hypoglycemic activity of RES is partly due to its α-glucosidase inhibitory effect in the small intestine.[14,15,19]

Recent studies suggested that these five bioactive components (DNJ, C3G, C3R, RES and OXY) could show varying degrees of α-glucosidase inhibitory activities. They may bind to different sites of α-glucosidase[20,21] competitively or noncompetitively like other inhibitors, inducing conformational changes[22,23] and reduction of activities. However, previous studies on DNJ, C3G, C3R and RES mainly deal with their individual inhibitory effects. No study has focused on their α-glucosidase inhibitory mechanisms, and there is no report indicating the differences of their inhibitory effects and mechanisms. In our lab, we had compared the contents of DNJ, C3G, C3R, RES and OXY in the mulberry leaves and fruits from 8 species in China.[16] Which of them is the most effective one? Whether their binding properties are different and their activities are affected by special intermolecular interactions? It will be significant to resolve these issues for

Received: May 3, 2013
Revised: July 24, 2013
Accepted: August 4, 2013
Published: August 5, 2013

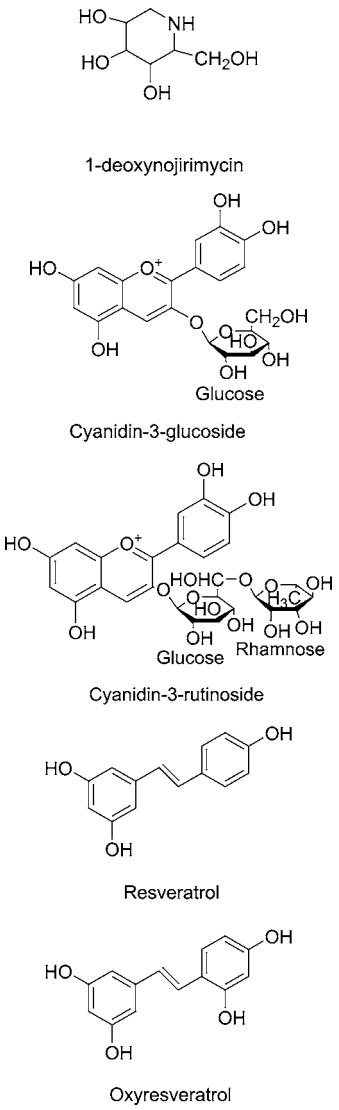

Figure 1. Chemical structures of 1-deoxynojirmycin, cyanidin 3-glucoside, cyanidin-3-rutinoside, resveratrol and oxyresveratrol.

the development of more powerful antidiabetic drugs and efficacious utilization of mulberry fruits and leaves.

In order to compare the α-glucosidase inhibitory mechanisms of DNJ, C3G, C3R, RES and OXY, we investigated their inhibitory effects and the interactions between ligands and α-glucosidase by enzymatic kinetics, fluorescence spectrophotometry (FS), and circular dichroism (CD). Homology modeling and docking studies were further employed to identify their binding properties.

MATERIALS AND METHODS

Chemicals. DNJ, C3G and C3R were purchased from Shanghai Yaji Biotechnology Co., Ltd. (Shanghai, China). Resveratrol was purchased from Jianfeng-Natural research and Development Co., Ltd. (Tianjin, China). Oxyresveratrol was isolated and purified in our lab with individual purity of no less than 98% as described by Song et al.[16] Bis-8-anilinonaphthalene-1-sulfonate (bis-ANS) and α-glucosidase (EC 3.2.1.20) from *Saccharomyces cerevisiae* were purchased from Sigma-Aldrich Chemical (St. Louis, MO, US). *p*-Nitrophenyl-α-D-glucopyranoside (PNPG) and reduced glutathione were purchased from Seebio biotechnology Co., Ltd. (Shanghai, China) Inc. All other chemicals were analytical reagent grade.

Measurement of α-Glucosidase Inhibitory Activity and Kinetics Assay. The assay uses PNPG as the substrate, which is hydrolyzed by α-glucosidase to release *p*-nitrophenol (PNP), a color agent that can be monitored at 405 nm.[24] Briefly, 20 μL DNJ, C3G, C3R, RES or OXY at different concentrations were combined with 40 μL of α-glucosidase (0.2 μM) and 20 μL of reduced glutathione (3 μM) in 20 mM sodium phosphate buffer (pH 6.8). After shaking for intensive mixing and incubation for 5 min at 37 °C, 20 μL of a 2.5 mM PNPG (2×10^4 μM) solution was added to start the reaction. After incubation at 37 °C for 10 min, 60 μL of sodium carbonate solution (200 μM) were added to stop the reaction, the total volume was 160 μL, and the released PNP was monitored at 405 nm by a Elx800 microplate reader (Biotek, USA). Acarbose was used as a positive control.

To further explore their inhibitory characteristic, the enzyme kinetic analysis was performed according to the above reaction using Lineweaver–Burk plots $1/v$ versus $1/[S]$. The quantity of α-glucosidase was maintained at 0.2 μM, and ligands (25–100 μM) were measured in various concentrations of PNPG (10^3–10^4 μM).

Intrinsic Fluorescence Measurements and Quenching Studies. α-Glucosidase (4 μM) was pretreated with 0–100 μM DNJ, C3G, C3R or 0–15 μM RES, OXY for 5 min at 25 or 37 °C. The intrinsic fluorescence spectra were measured with a Cary Eclipse fluorescence spectrophotometer equipped with a temperature controller (Agilent, USA). The excitation wavelength (λ_{ex}) was 280 nm, and emission (λ_{em}) spectra were acquired by scanning from 300 to 500 nm. All measurements were performed at 25 and 37 °C.[25] The dynamic quenching constant (K_{sv}) and the rate constant in the process of double molecular quenching (K_q) were calculated by plotting F_0/F versus $[Q]$ according to the Stern–Volmer eq 1 as follows:[26]

$$F_0/F = 1 + K_{SV}[Q] = 1 + K_q t_0[Q] \quad (1)$$

where F_0 and F are the fluorescence intensity of α-glucosidase in the presence or absence of different quenchers, $[Q]$ is the concentration of quenchers, and t_0 ($\approx 10^{-8}$ s) is the average life of the fluorescent molecule without quencher.

The fluorescence intensity was determined by the quencher concentration through eq 2. The binding constant (K_A) and binding sites (n) at 25 or 37 °C were obtained through the plots of $\lg[(F_0 - F)/F]$ versus $\lg[Q]$.

$$\lg(F_0 - F)/F = \lg K_A + n\lg[Q] \quad (2)$$

In eq 2, F_0 and F are the fluorescence intensity of α-glucosidase in the presence or absence of different quenchers, $[Q]$ is the concentration of quenchers.

Thermodynamic parameters ΔH and ΔS (changes in enthalpy and entropy) were calculated by the following thermodynamic equations, where K, K_1 and K_2 value was obtained by the above calculation.

$$\Delta G = \Delta H - T\Delta S \quad (3)$$

$$\Delta G = -RT\ln K \quad (4)$$

$$\ln(K_2/K_1) = (1/T_1 - 1/T_2)\Delta H/R \quad (5)$$

The interactions between ligands and protein belong to weak intermolecular forces, including van der Waals force, hydrogen bonding, electrostatic attraction, hydrophobic interaction and so on. More specifically, if $\Delta H > 0$ and $\Delta S > 0$, the main force would be a hydrophobic force; if $\Delta H < 0$ and $\Delta S < 0$, it would be hydrogen bonding; if $\Delta H < 0$ and $\Delta S > 0$, it would be an electrostatic force.

Hydrophobic Analysis of α-Glucosidase Using Bis-ANS. α-Glucosidase (2 μM) was incubated in the presence of certain concentrations of compounds (0, 40, 120 μM) at 37 °C for 5 min. Bis-ANS (5 μM) was then added, and fluorescence was measured after incubation at 37 °C for 5 min (λ_{ex} = 400 nm, λ_{em} = 450–600 nm) using a Synergy^{Mx} multifunctional microplate detector (Biotek, USA).

Circular Dichroism (CD) Assay. Far UV CD spectra (190–240 nm) of α-glucosidase (2 μM) treated with DNJ, C3G, C3R, RES or OXY (0, 40, 120 μM) was measured at 37 °C with a circular spectrometer (Applied Photophysics, England). The spectra were

collected and corrected by subtraction of a blank containing 2×10^4 μM potassium phosphate buffer (pH 6.8), reduction of noise, and smoothing. Secondary structure estimations were based on the far-UV CD spectra of α-glucosidase according to the method of SOMCD[27] (using the SOMCD neural network algorithm, http://geneura.ugr.es/cgi-bin/somcd/index.cgi).

Molecular Modeling and Docking. A 38% sequence identity and 59% residues similarity between *Saccharomyces cerevisiae* α-glucosidase and *Bacillus cereus* oligo-1,6-glucosidase exists. The three-dimensional (3D) homology model of α-glucosidase was constructed based on the crystal structure of *B. cereus* oligo-1,6-glucosidase (PDB ID: 1UOK). This step was performed using Easymodeller (v 2.0), a graphical user interface for the program Modeler (v 9.11), and the homology model was further optimized. The final protein model was validated by PROCHECK (using the online structural analysis and verification server http://nihserver.mbi.ucla.edu/SAVES/).

The docking analysis was carried out by means of the Autodock tools (ADT) v1.5.4 and autodock v4.2 program (Autodock, Autogrid, Autotors, and Copyright-1991e2000). All ligands were first docked to the active site comprised of Asp214, Glu276 and Asp349. The search was carried out with the Lamarckian Genetic Algorithm and extended over the whole receptor protein used as blind docking, in 250 individuals. The remaining parameters were set as default. A cluster analysis based on root-mean-square deviation values, with reference to the starting geometry, was subsequently performed, and the lowest energy conformation of the more populated cluster was considered as the most reliable solution.

Data Presentation and Statistical Analysis. All of the experiments were repeated at least three times, and essentially, the same results were obtained. The data for the α-glucosidase inhibitory activities are presented as mean ± standard deviations (SD). Typical spectra and data were presented as figures.

RESULTS

Comparison of α-Glucosidase Inhibitory Activities by Ligands. As shown in Table 1, the α-glucosidase inhibitory sequence was OXY > DNJ > RES > acarbose > C3G > C3R. The values of IC_{50} were 35.62, 60.75, 32.80, and 229.80 μM for DNJ, RES, OXY and acarbose respectively, while IC_{50} values of C3G and C3R were larger than 1×10^3 μM. The result indicated that DNJ, RES and OXY were effective α-glucosidase inhibitors.

Table 1. IC_{50} Values of α-Glucosidase Inhibitory Effect and Inhibitory Types

ligands	IC_{50} (μM)	type of inhibition
DNJ	35.62 ± 1.40	competive
C3G	>1000	mix type
C3R	>1000	mix type
RES	60.75 ± 1.90	noncompetive
OXY	32.80 ± 0.96	noncompetive
acarbose	229.80 ± 1.19	competive

To further explore the inhibitory characteristics of these compounds, the kinetic assay was performed using Lineweaver–Burk plots $1/v$ versus $1/[S]$ (Figure 2). A Lineweaver–Burk plot of DNJ generated straight lines which had intersections on the *Y*-axis, indicating that the type of inhibition was a competitive mode. C3G and C3R had no intersection on the axis (data not shown), indicating the type of inhibition was a mixed competitive and noncompetitive type. Otherwise, the straight lines of OXY intersected on the *X*-axis (Figure 2), indicating that the type of inhibition was noncompetitive which was consistent with the results of the RES.

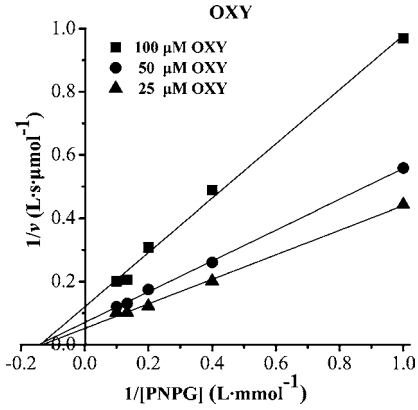

Figure 2. Lineweaver–Burk plots of the inhibition kinetics of α-glucosidase by OXY. α-Glucosidase (0.2 μM) was incubated with 25–100 μM OXY at 37 °C for 5 min. The concentrations of PNPG were 1, 2.5, 5, 7.5 and 10×10^3 μM.

Comparison of Intrinsic Fluorescence Quenching Effects Induced by Ligands. As shown in Figure 3A and Figure 4, α-glucosidase had a fluorescence peak at 337 nm, which mainly belonged to Trp residues of α-glucosidase. However, while incubated with different ligands, the fluorescence intensity was quenched gradually with the increasing concentrations of ligands. The quenching effect of OXY was the strongest, followed by RES, C3G, C3R, and DNJ. There were significant differences between their quenching spectra. When the concentration of ligands reached 100 μM, DNJ slightly changed the spectrum (Figure 3A) while C3G and C3R almost completely quenched their spectra (Figure 4A, B). When the temperature was increased to 37 °C, their quenching spectra were not affected by temperature significantly (data not shown). RES and OXY could quench α-glucosidase fluorescence at a concentration of less than 15 μM (Figure 4C, E). Interestingly, there were concomitant increases in the fluorescence emission at 430 and 410 nm with the addition of RES and OXY (Figure 4C–F) respectively which may indicate the energy transfer between ligands and protein. The increasing rate of RES and OXY fluorescence emission was slowed down by the increasing temperature (Figure 4D, F). Moreover, there was a significant λ_{em} red shift with the addition of RES. The results obtained from the fluorescence spectra clearly showed that interactions between ligands (DNJ, C3G, C3R, RES and OXY) and α-glucosidase had occurred, and the interactions had resulted in variation for Trp residues.

Mechanism of Fluorescence Quenching. To further study the properties of interactions between ligands and α-glucosidase, the dynamic quenching constant (K_{sv}) and the rate constant in the process of double molecular quenching (K_q) were calculated by plotting F_0/F versus $[Q]$ (Figure 3B) according to the fluorescence quenching theory.[26,28] For RES and OXY, the values of K_q (Table 2, at both 25 and 37 °C) were much greater than 2.0×10^{10} per mol/s, so we ensured that the quenching of RES and OXY belonged to static quenching. As showed in Table 2, the K_{sv} values of DNJ, RES and OXY were decreased with increasing temperature ($K_{sv\ 25} > K_{sv\ 37}$). Therefore, DNJ, RES and OXY induced quenching were evaluated as static quenching by forming a ligand-α-glucosidase complex. For C3G and C3R (Table 2), the rise in temperature led to an increase in the formation constant (K_{sv}). Therefore, quenching processes of C3G and C3R were dynamic quenching induced by the collision of molecules.

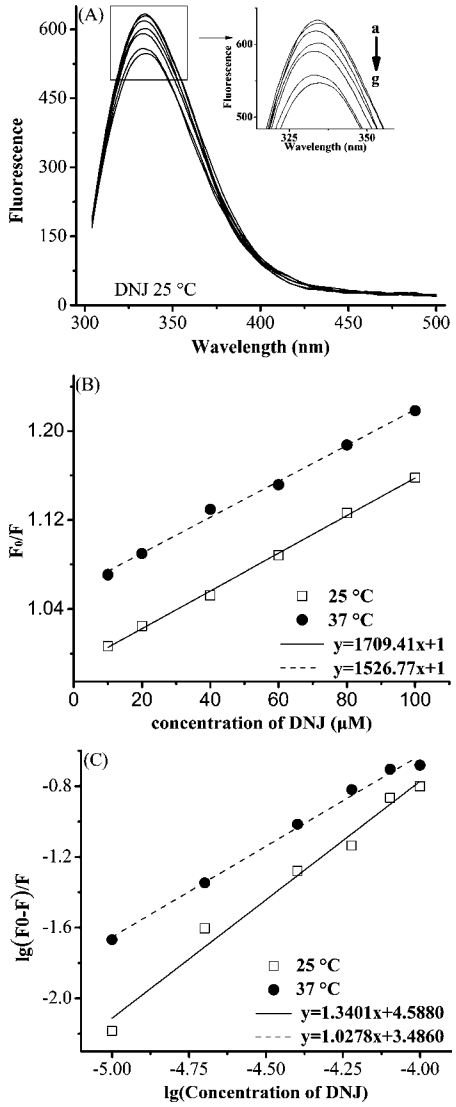

Figure 3. Intrinsic fluorescence quenching induced by DNJ. (A) Intrinsic fluorescence spectra changes of α-glucosidase by DNJ at 25 °C. α-Glucosidase (4 μM) was incubated with DNJ (0−100 μM) at 25 and 37 °C for 5 min. Spectra were acquired from 300 to 500 nm. (a−g) 4 μM α-glucosidase in the presence of 0, 10, 20, 40, 60, 80 and 100 μM. (B) Stern−Volmer plots of DNJ to α-glucosidase based on fluorescence quenching at 25 and 37 °C. (C) Plots of lg[$(F_0 - F)/F$] versus lg[Concentration of (DNJ)].

Binding Constants (K_A) and Binding Sites (n). The binding constants (K_A) and number of binding sites (n) were obtained through the plots of lg[$(F_0 - F)/F$] versus lg[Q] (Figure 3C). The results (Table 2) showed that the sequence of binding constants (K_A) at 37 °C was C3R > C3G > DNJ > RES > OXY. The number of binding sites (n) of DNJ, RES and OXY were close to 1.34, 0.82, and 0.74 at 25 °C respectively, but decreased when the temperature reached 37 °C. The binding sites of C3G and C3R increased with the temperature which was consistent with their dynamic quenching.

Thermodynamics of Interaction between Ligands and α-Glucosidase. As seen from Table 3, the ΔG values of ligands were all negative; it meant that the interactions between ligands and α-glucosidase were a spontaneous process of entropy increasing and free energy decreasing. According to the change in relative values for enthalpy and entropy (ΔH and ΔS), interactions between DNJ, RES, OXY and α-glucosidase were mainly driven by hydrophobic force ($\Delta H > 0$ and $\Delta S > 0$), while C3G and C3R was mainly driven by hydrogen bonding ($\Delta H < 0$ and $\Delta S < 0$, Table 3).

Hydrophobicity Changes of α-Glucosidase Induced by Ligands. Bis-ANS is a useful fluorescence probe in measuring the surface hydrophobicity change of proteins due to its own characteristic.[29] The relative fluorescence intensities (λ_{ex} = 400 nm, λ_{em} = 450−600 nm) were obtained and are shown in Figure 5. With increasing concentrations of these components, the bis-ANS-enzyme fluorescence was reduced. The surface hydrophobicity changes induced by C3G and C3R (Figure 5B) were stronger than those of other ligands (Figure 5A, C). These results suggested that all ligands could reduce the hydrophobic surface of α-glucosidase.

Conformation Changes of α-Glucosidase Induced by Ligands. In order to study the influence of ligands on the secondary structure of α-glucosidase, CD spectra of α-glucosidase (190−240 nm) were acquired. The CD spectra of α-glucosidase exhibited two negative bands in the 208 and 222 nm (Figure 6A−C), which were spectral features of a protein rich in α-helix structure. Analysis of the CD spectra of α-glucosidase using SOMCD online predicted that the α-helix content was 37.9% and the β-sheet content was 23.5% respectively. When α-glucosidase was incubated with different ligands, the CD spectra were shifted and showed an increase in the percentage of α-helix and decline in the percentage of β-sheet (Table 4). DNJ and OXY (120 μM) were the most efficient compounds to alter the secondary structure of the protein (Figure 6A, C) which made the α-helix content increase to 42.7 and 43.7% respectively. Relatively, C3G had little effect on the conformation of glucosidase (data not shown). These results suggested that interactions between ligands and α-glucosidase could induce changes in the secondary structure of α-glucosidase.

Protein 3D Structure Generation and Molecular Docking. As the α-glucosidase inhibitory analysis of our research was carried out on *S. cerevisiae*, it would be appropriate to investigate the binding mode of ligands with the *S. cerevisiae* structure. Unfortunately the 3D structure of the protein is not available so far, and hence a homology modeled structure was constructed based on the *B.cereus* oligo-1,6-glucosidase[30]- (Figure 7). The evaluation results of PROCHECK show that 88.8%, 9.9% and 1.0% of the residues are located within the most favorable, additionally allowed and generously allowed regions of the Ramachandran plot, respectively. This result suggested that the homology modeled was suitable for docking study.

As shown in Figure 8A, DNJ completely occupied the active center which was formed by ASP214, GLU276 and ASP349.[31] The ASP68 and ARG439 residues helped form the hydrophobic pocket. Two more residues, HIS111 and HIS348 of *S.cerevisiae* glucosidase, which may be involved in substrate binding could also form hydrogen bonds with DNJ. This is consistent with recent computational studies that showed DNJ can interact with the active center of acid α-glucosidase.[32] In the case of RES and OXY (Figure 8B−C), it could be seen that a new hydrophobic patch comprising PHE318, THR319, PHE357 and PHE540 along with ARG356 surrounded and held the ligands. This hydrophobic pocket was completely different from the active center and was suggested to be a new binding site which had not been reported before (Figure 7). Interestingly, we also found a fluorescent residue TRP323

dx.doi.org/10.1021/jf4019323 | J. Agric. Food Chem. 2013, 61, 8110−8119

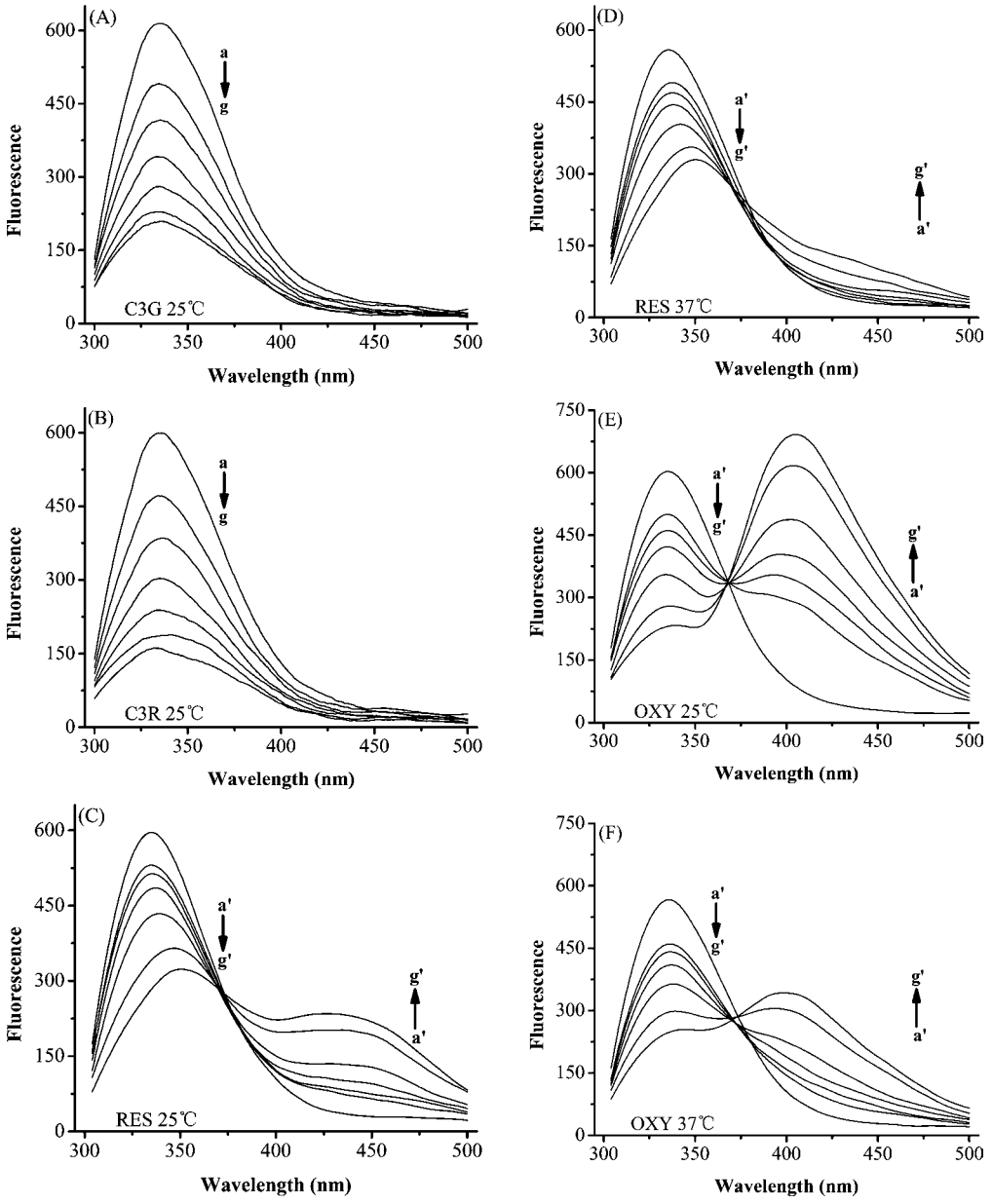

Figure 4. Intrinsic fluorescence quenching induced by C3G, C3R, RES, and OXY. α-Glucosidase (4 μM) was incubated with C3G, C3R (0−100 μM), RES, or OXY (0−15 μM) at 25 and 37 °C for 5 min. Spectra were acquired from 300 to 500 nm. (A−B) Fluorescence spectra changes of α-glucosidase by C3G and C3R at 25 °C. (a−g) 4 μM α-glucosidase in the presence of 0, 10, 20, 40, 60, 80 and 100 μM C3G or C3R. (C−D) Spectra changes induced by RES at 25 and 37 °C. (E−F) Spectra changes induced by OXY at 25 and 37 °C. (a′−g′) 4 μM α-glucosidase in the presence of 0, 1, 1.5, 2.5, 5, 10 and 15 μM RES or OXY.

Table 2. Constants/Parameters Obtained from the Intrinsic Fluorescence Data

ligands	T (°C)	K_{sv} (L/mol)	$K_q/10^{11}$ (L/mol/s)	$K_A/10^3$ (L/mol)	binding (n)
DNJ	25	1709.41	1.71	38.72	1.34
	37	1526.77	1.53	3.06	1.03
C3G	25	18021.49	18.02	7.05	0.89
	37	19860.36	19.86	14.54	0.97
C3R	25	28332.46	28.33	24.33	0.99
	37	39769.00	39.77	77.97	1.10
RES	25	68761.62	68.76	9.54	0.82
	37	53888.12	53.89	2.49	0.69
OXY	25	85055.18	85.06	5.88	0.74
	37	63910.22	63.91	1.31	0.63

Table 3. Thermodynamic Parameters of Interaction between α-Glucosidase and Ligands

ligands	T (°C)	ΔH (kJ/mol)	ΔS (J/mol/K)	ΔG (kJ/mol)
DNJ	25	162.58	633.12	−26.19
	37			−20.70
C3G	25	−46.37	−81.85	−21.97
	37			−24.72
C3R	25	−74.61	−166.28	−25.04
	37			−29.05
RES	25	86.12	365.04	−22.72
	37			−20.16
OXY	25	96.22	394.87	−21.52
	37			−18.51

dx.doi.org/10.1021/jf4019323 | J. Agric. Food Chem. 2013, 61, 8110−8119

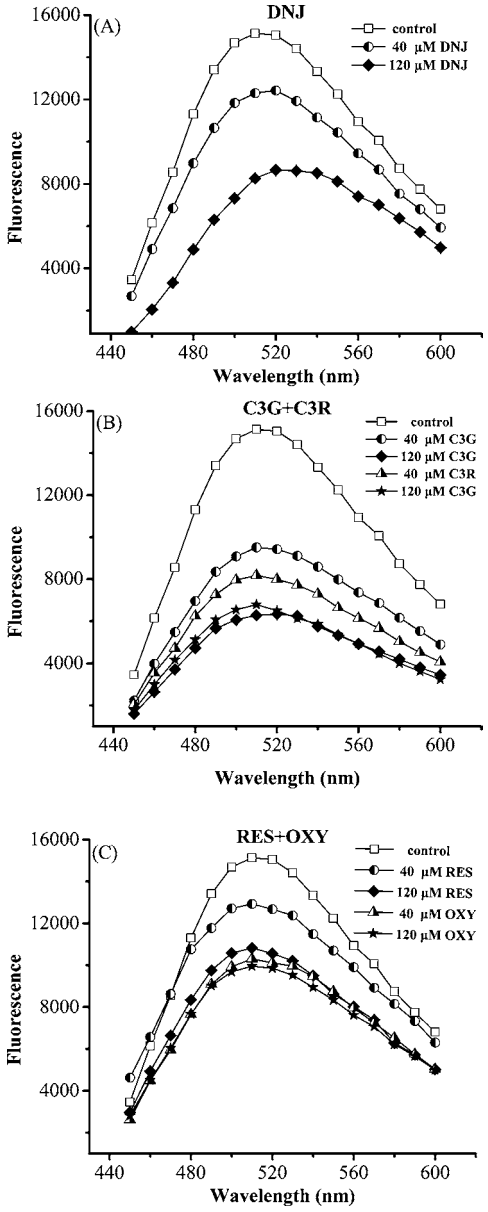

Figure 5. Changes of α-glucosidase-bis-ANS complex fluorescence by ligands. α-Glucosidase (2 μM) was incubated with DNJ, C3G, C3R RES, and OXY (0, 40 and 120 μM) at 37 °C for 5 min. Bis-ANS (5 μM) was then added, and fluorescence from 450 to 600 nm was measured after incubation at 37 °C for 5 min. (A–C) 2 μM α-glucosidase in the presence of DNJ (A), C3G and C3R (B), and RES and OXY (C) respectively.

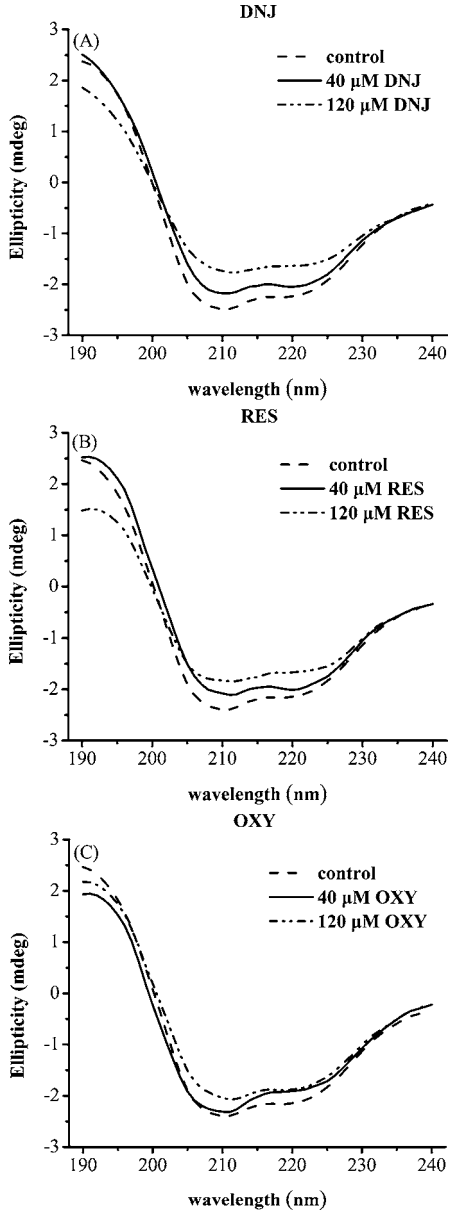

Figure 6. CD spectra of α-glucosidase in the absence or presence of ligands. α-Glucosidase (2 μM) was incubated with DNJ, C3G, C3R, RES, or OXY (0, 40, 120 μM) for 5 min at 37 °C. Spectra were acquired from 190 to 240 nm. 2 μM α-glucosidase in the presence of DNJ (A), RES (B), or OXY(C) respectively.

which may be the source of the endogenous fluorescence which was near the pocket. When we chose a tolerance of 2.0, the conformations of the C3G-glucosidase or C3R-glucosidase complex scattered and no populated cluster was found. So we changed the tolerance to 5.0 and found that C3G could be exposed to both the active center and binding site (Figure 8D, E) with equal probability. The glycosyl of C3G could be exposed to the active center and form hydrogen bonds with ASP214 and ASP349 (Figure 8D). While aglycon formed hydrogen bonds with LEU176, VAL277 and SER244, C3G could also be exposed to the binding site and form hydrogen bonds with GLY306, PHE357, ALA358 and ARG356 (Figure 8E). These results suggested that five ligands could act with glucosidase at different sites and the differences between their

Table 4. Secondary Structure Changes of α-Glucosidase Influenced by Ligands

ligands	α-helix (%)	β-fold (%)	β-turn (%)	random (%)
control	37.9 ± 2.5	23.5 ± 5	10.3 ± 2.3	28.3 ± 3.5
40 μM DNJ	41.6 ± 3.4	14.6 ± 6.7	14 ± 3.2	29.9 ± 6.3
120 μM DNJ	42.7 ± 6.4	13.9 ± 7.1	16.9 ± 2.7	26.0 ± 2.5
40 μM C3G	38.1 ± 1.2	23.6 ± 4	10.2 ± 2.3	28.1 ± 3.5
120 μM C3G	38.5 ± 2.4	23 ± 2.2	11.1 ± 2.3	27.4 ± 3.2
40 μM C3R	41.5 ± 3.2	15 ± 6.4	14.2 ± 3	29.4 ± 6.1
120 μM C3R	41.6 ± 6.4	16.5 ± 13.5	13.3 ± 3.2	28.6 ± 5.6
40 μM RES	39.9 ± 1.7	14 ± 2.3	9 ± 2.3	27.2 ± 1.7
120 μM RES	41.5 ± 3.2	15 ± 6.4	14.2 ± 3	29.4 ± 6.1
40 μM OXY	41.6 ± 6.4	16.5 ± 3.5	13.3 ± 3.2	28.6 ± 5.6
120 μM OXY	43.7 ± 6.4	13.7 ± 7.1	16 ± 2.7	26.4 ± 2.5

dx.doi.org/10.1021/jf4019323 | J. Agric. Food Chem. 2013, 61, 8110–8119

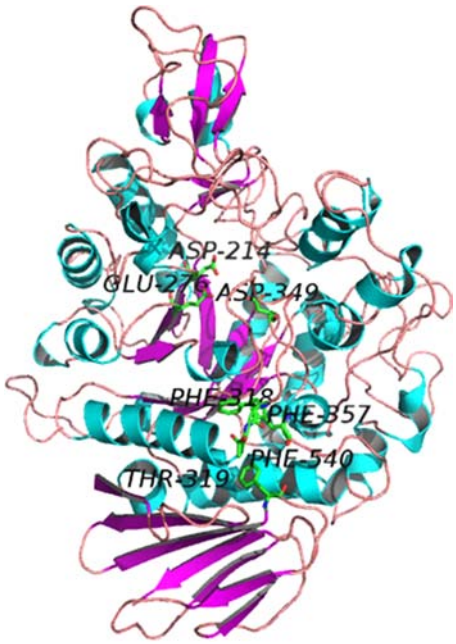

Figure 7. Ribbon diagram of the homology model of α-glucosidase. The homology model of *Saccharomyces cerevisiae* α-glucosidase was constructed based on the crustal structure of *Bacillus cereus* oligo-1, 6-glucosidas. The model was colored by secondary structures.

fluorescence quenching spectra were mainly due to their binding properties.

DISCUSSION

Mulberry (*Morus, Moraceae*) plants are distributed widely in China, and at least 15 species of mulberry are recognized. Production and consumption of mulberry juices, fruits, and leaves are increasing rapidly because of their potential for treating diabetes mellitus. In our lab, we had compared the contents of DNJ, C3G, C3R, RES and OXY in the mulberry leaves or fruits from 8 species in China.[16]

In this study, we compared the α-glucosidase inhibitory effects of five bioactive components (DNJ, C3G, C3R, RES and OXY) contained in mulberry plants. The α-glucosidase inhibitory ability of OXY, which was identified as a new inhibitor for the first time, was similar to DNJ and RES. Since these five ligands had different molecule structures, their inhibitory mechanisms were different. DNJ could hinder the binding of the substrate to the enzyme competitively. However, RES and OXY may affect the enzyme activity in another way. First, they might combine with the enzyme and then change the conformation. According to these results, we suggested that they might interact with the enzyme at different sites and should have different binding properties.

By comparing the fluorescence quenching spectra, three completely different types of quenching spectra were observed. The intrinsic fluorescence of α-glucosidase is mainly generated from tryptophan, which presents in the binding domain of α-glucosidase rather than the catalytic domain.[33] Therefore, we suggested that DNJ could bind to the catalytic domain[20] resulting in weak quenching, while RES and OXY could bind to the binding domain. C3G and C3R might also interact with the same binding domain. These assumptions were further verified in the docking study (Figures 7 and 8A–E). The concomitant increases in the fluorescence emission at 430 and 410 nm with the addition of RES and OXY (Figure 4C–F) respectively indicated the characteristic wavelength of the bound-protein and possible energy transfer.[32] This phenomenon was similar to other relevant ligand–protein interaction studies.[34,35] Moreover, the λ_{em} red shift with the addition of RES indicated that the binding of RES to α-glucosidase changed the microenvironment of Trp.[35] The results obtained from the fluorescence spectra clearly showed us that the interactions between ligands (C3G, C3R, RES and OXY) and α-glucosidase had resulted in significant variations for Trp residues or conformational changes.

According to the quenching theory, the quenching mechanisms of DNJ, RES and OXY included static quenching which could induce the formation of complexes. These phenomena were similar to other potent α-glucosidase inhibitors, for example, quercetin, isoquercetin[28] and butyl-isobutyl-phthalate (BIP),[22] all of which formed a stable complex. In the case of DNJ, it could show similar affinity toward α-glucosidase compared with acarbose.[36] It may suggest that ligands might show a stronger inhibitory effect if they can combine with the enzyme molecules to induce strong intermolecular interactions. Compared with other inhibitors,[22,28,37] the K_A values of C3G and C3R were larger. This might be due to their glycoside, especially the diglucoside of C3R. It seemed that the main driving force was also impacted by the glycosides. When aglycone was glycosides-linked, the intermolecular hydrophobic force between ligands and α-glucosidase was weakened, accompanied by the reduction of their α-glucosidase inhibitory effects.

The hydrophobicity surface is an important factor in the formation of the enzyme active center. All ligands could induce changes in the hydrophobic surface as well as the intrinsic fluorescence. These results were consistent with the effects of other inhibitors. It suggested that a poor hydrophobic surface usually hindered the formation of an active center in the enzyme molecules.[22,23] The increase in α-helix induced by our components was similar to other α-glucosidase inhibitors, including bis(2,3-dibromo-4,5-dihydroxybenzyl) (BDDE), which also induced an increase in the α-helix content.[23] However, these compounds induced conformational changes that were opposite to those of other inhibitors, such as BIP,[22] curcuminoids analogs[38] and genistein.[39] The reason is that α-glucosidase, a member of the glycoside hydrolase family 13 (GH13), is composed of three domains: a catalytic domain folded in a $(\beta/\alpha)_8$ barrel in the N-terminal, a subdomain and a β-sheet rich domain in the C-terminus.[40] The α-helix content of α-glucosidase should be the decisive factor. Slight changes in the α-helix content will attenuate the activity of the enzyme.

In our docking study, we found that these ligands could bind to α-glucosidase at different sites. DNJ could completely occupy the active center. This hydrophobic pocket which contains ASP68 and ARG439 is different from the pocket of acarbose binding comprising TYR71, PHE157 and PHE177.[41] We also found a new binding site comprised of PHE318, THR319, PHE357 and PHE540 along with ARG356, which are in surrounding positions, that is different from the active center (Figure 7). The predicted binding site in our study may provide a novel approach for developing and designing novel α-glucosidase inhibitors. In the case of C3G and C3R, cluster analysis showed that different conformations of ligand–glucosidase complexes occur at the same rate. This result supported previous research that the interactions between C3G, C3R and glucosidase were mainly driven by the collision of

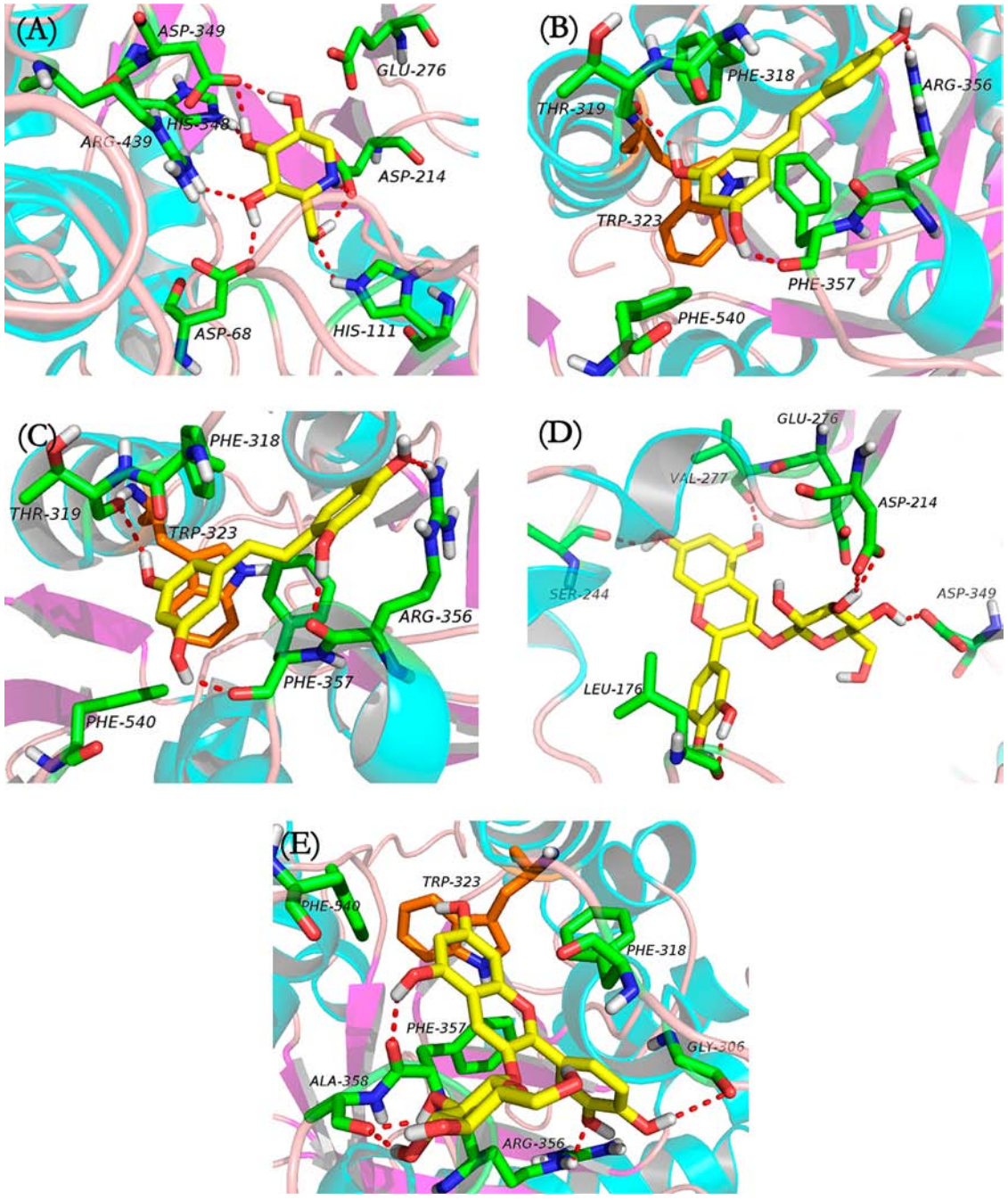

Figure 8. Docking model predicted structural details of DNJ, RES, OXY and C3G. The docking study was carried out by using Autodock tools (ADT) v1.5.4 and autodock v4.2 program. (A and D) Hydrogen-bonding network of DNJ and C3G at active center; (B, C, and E) hydrogen-bonding network of RES, OXY, and C3G at binding site.

molecules. Moreover, it suggested that the TRP323 residue was the source of α-glucosidase endogenous fluorescence. These results suggested that five ligands could bind to glucosidase at different sites and the differences between their fluorescence quenching spectra were mainly due to the TRP323 residue.

It is easy to distinguish these bioactive components from other commercial drugs, such as miglitol and voglibose, which are confined to glycosidic derivatives and belong to competitive inhibitors. In recent years, mulberry leaf tea has attracted attention in various Asian countries, as it is claimed to be rich in DNJ. Mulberry tea when heated for 3−5 min in boiling water (98 °C) could inhibit the activity of α-glucosidase[42] effectively. Since the presence of anthocyanins is universally associated with the attractive color and beneficial biological activities, the C3G and C3R are logical candidates for food colorants.[43] RES and OXY are compounds that are structurally different from the glycoside derivatives and belong to noncompetitive inhibitors. Theoretically, their inhibition effects are not affected by a high concentration of carbohydrates.[22] Moreover, RES and OXY may also interact with other proteins (*p*-glycoprotein and MRPs) to cross small intestinal cells due to their nonspecific binding properties.[44] Therefore, RES and OXY could be developed as a new type of hypoglycemic agent to act simultaneously in the small intestine and even in vivo.

In summary, we have compared the inhibitory effects of five bioactive components (DNJ, C3G, C3R, RES and OXY) and

dx.doi.org/10.1021/jf4019323 | J. Agric. Food Chem. 2013, 61, 8110−8119

acarbose toward α-glucosidase's activity and have provided insight into understanding the interaction between different inhibitors and α-glucosidase using spectroscopy methods. This work suggests that DNJ and OXY are major hypoglycemic ingredients in mulberry leaves. C3G and C3R are the most abundant components in the mulberry fruits. They can delay the postprandial rise in blood glucose to prevent diabetes mellitus and, therefore, could be potentially used as general food-based hypoglycemic agents. This study also identifies OXY as a novel and potent α-glucosidase inhibitor; further in vivo and in vitro studies related to its antidiabetes metabolism need to be investigated.

■ ASSOCIATED CONTENT

Supporting Information

Lineweaver−Burk plots of the inhibition kinetics of α-glucosidase by DNJ, C3G, C3R, and RES were shown in supplemental Figure 1. The fluorescence quenching spectra of α-glucosidase in the presence of DNJ, C3G, C3R at 37 °C were shown in supplemental Figure 2. CD spectra of α-glucosidase in the absence or presence of C3G and C3R were shown in supplemental Figure 3. This material is available free of charge via the Internet at http://pubs.acs.org.

■ AUTHOR INFORMATION

Corresponding Author

*Phone: +86-21-64251185. Fax: +86-21-64251185. E-mail: luyanhua@ecust.edu.cn.

Notes

The authors declare no competing financial interest.

■ ACKNOWLEDGMENTS

This work was supported by "the Fundamental Research Funds for the Central Universities", and partially supported by Shanghai Leading Academic Discipline Project (B505), the National Special Fund for State Key Laboratory of Bioreactor Engineering (2060204).

■ ABBREVIATIONS USED

PNPG, *p*-nitrophenyl-α-D-glucopyranoside; PNP, *p*-nitrophenol; DNJ, 1-deoxynojirimycin; C3G, cyanidin-3-glucoside; C3R, cyanidin-3-rutinoside; RES, resveratrol; OXY, oxyresveratrol; bis-ANS, Bis-8-anilinonaphthalene-1-sulfonate; min, minutes

■ REFERENCES

(1) Bastyr, E. J.; Stuart, C. A.; Brodows, R. G.; Schwartz, S.; Graf, C. J.; Zagar, A.; Kenneth, R. Therapy Focused on Lowering Postprandial Glucose, Not Fasting Glucose, May Be Superior for Lowering. *Diabetes Care* **2000**, *23*, 1236−1241.

(2) American Diabetes Assocition Postprandial Blood Glucose. *Diabetes Care* **2001**, *24*, 775−778.

(3) Trial, T. S.; Josse, R. G.; Gomis, R. Acarbose Treatment and the Risk of Cardiovascular Disease and Hypertension. *J. Am. Med. Assoc.* **2003**, *290*, 486−494.

(4) Kawamori, R.; Tajima, N.; Iwamoto, Y.; Kashiwagi, A.; Shimamoto, K.; Kaku, K. Voglibose for prevention of type 2 diabetes mellitus: a randomised, double-blind trial in Japanese individuals with impaired glucose tolerance. *Lancet* **2009**, *373*, 1607−1614.

(5) Hsiao, S.-H.; Liao, L.-H.; Cheng, P.-N.; Wu, T.-J. Hepatotoxicity associated with acarbose therapy. *Ann. Pharmacother.* **2006**, *40*, 151−154.

(6) Tao, W.; Deqin, Z.; Yuhong, L.; Hong, L.; Zhanbiao, L.; Chunfeng, Z.; Limin, H.; Xiumei, G. Regulation effects on abnormal glucose and lipid metabolism of TZQ-F, a new kind of Traditional Chinese Medicine. *J. Ethnopharmacol.* **2010**, *128*, 575−582.

(7) Kim, G.-N.; Kwon, Y.-I.; Jang, H.-D. Mulberry leaf extract reduces postprandial hyperglycemia with few side effects by inhibiting α-glucosidase in normal rats. *J. Med. Food* **2011**, *14*, 712−717.

(8) Park, J. M.; Bong, H. Y.; Jeong, H. I.; Kim, Y. K.; Kim, J. Y.; Kwon, O. Postprandial hypoglycemic effect of mulberry leaf in Goto-Kakizaki rats and counterpart control Wistar rats. *Nutr. Res. Pract.* **2009**, *3*, 272−278.

(9) Nakagawa, K.; Kubota, H.; Kimura, T.; Yamashita, S.; Tsuzuki, T.; Oikawa, S.; Miyazawa, T. Occurrence of orally administered mulberry 1-deoxynojirimycin in rat plasma. *J. Agric. Food Chem.* **2007**, *55*, 8928−8933.

(10) Kimura, T.; Nakagawa, K.; Kubota, H.; Kojima, Y.; Goto, Y.; Yamagishi, K.; Oita, S.; Oikawa, S.; Miyazawa, T. Food-grade mulberry powder enriched with 1-deoxynojirimycin suppresses the elevation of postprandial blood glucose in humans. *J. Agric. Food Chem.* **2007**, *55*, 5869−5874.

(11) Nuengchamnong, N.; Ingkaninan, K.; Kaewruang, W.; Wongareonwanakij, S.; Hongthongdaeng, B. Quantitative determination of 1-deoxynojirimycin in mulberry leaves using liquid chromatography-tandem mass spectrometry. *J. Pharm. Biomed. Anal.* **2007**, *44*, 853−858.

(12) Yasuda, K.; Kizu, H.; Yamashita, T.; Kameda, Y.; Kato, A.; Nash, R. J.; Fleet, G. W. J.; Molyneux, R. J.; Asano, N. New sugar-mimic alkaloids from the pods of Angylocalyx pynaertii. *J. Nat. Prod.* **2002**, *65*, 198−202.

(13) Kuriyama, C.; Kamiyama, O.; Ikeda, K.; Sanae, F.; Kato, A.; Adachi, I.; Imahori, T.; Takahata, H.; Okamoto, T.; Asano, N. In vitro inhibition of glycogen-degrading enzymes and glycosidases by six-membered sugar mimics and their evaluation in cell cultures. *Bioorg. Med. Chem.* **2008**, *16*, 7330−7336.

(14) Palsamy, P.; Subramanian, S. Chemico-Biological Interactions Modulatory effects of resveratrol on attenuating the key enzymes activities of carbohydrate metabolism in streptozotocin −nicotinamide-induced diabetic rats. *Chem.-Biol. Interact.* **2009**, *179*, 356−362.

(15) Kerem, Z.; Bilkis, I.; Flaishman, M.; Sivan, L. Antioxidant Activity and Inhibition of α-Glucosidase by trans-Resveratrol, Piceid, and a Novel trans-Stilbene from the Roots of Israeli Rumex bucephalophorus L. *J. Agric. Food Chem.* **2006**, *54*, 1243−1247.

(16) Song, W.; Wang, H.-J.; Bucheli, P.; Zhang, P.-F.; Wei, D.-Z.; Lu, Y.-H. Phytochemical profiles of different mulberry (Morus sp.) species from China. *J. Agric. Food Chem.* **2009**, *57*, 9133−9140.

(17) Akkarachiyasit, S.; Charoenlertkul, P.; Yibchok-Anun, S.; Adisakwattana, S. Inhibitory Activities of Cyanidin and Its Glycosides and Synergistic Effect with Acarbose against Intestinal α-Glucosidase and Pancreatic α-Amylase. *Int. J. Mol. Sci.* **2010**, *11*, 3387−3396.

(18) Sirichai, A.; Sirintorn, Y.-A.; Piyawan, C.; Natthakan, W. Cyanidin-3-rutinoside alleviates postprandial hyperglycemia and its synergism with acarbose by inhibition of intestinal α-glucosidase. *J. Clin. Biochem. Nutr.* **2011**, *49*, 36−41.

(19) Chen, W.-P.; Chi, T.-C.; Chuang, L.-M.; Su, M.-J. Resveratrol enhances insulin secretion by blocking K(ATP) and K(V) channels of beta cells. *Eur. J. Pharmacol.* **2007**, *568*, 269−277.

(20) Bharatham, K.; Bharatham, N.; Park, K. H.; Lee, K. W. Binding mode analyses and pharmacophore model development for sulfonamide chalcone derivatives, a new class of α-glucosidase inhibitors. *J. Mol. Graphics Modell.* **2008**, *26*, 1202−1212.

(21) Yao, X.; Mauldin, R.; Byers, L. Multiple sugar binding sites in α-glucosidase. *Biochim. Biophys. Acta* **2003**, *1645*, 22−29.

(22) Liu, M.; Zhang, W.; Qiu, L.; Lin, X. Synthesis of butyl-isobutyl-phthalate and its interaction with α-glucosidase in vitro. *J. Biochem.* **2011**, *149*, 27−33.

(23) Liu, M.; Zhang, W.; Wei, J.; Lin, X. Synthesis and α-glucosidase inhibitory mechanisms of bis(2,3-dibromo-4,5-dihydroxybenzyl) ether, a potential marine bromophenol α-glucosidase inhibitor. *Mar. Drugs.* **2011**, *9*, 1554−1565.

(24) You, Q.; Chen, F.; Wang, X.; Luo, P. G.; Jiang, Y. Inhibitory effects of muscadine anthocyanins on α-glucosidase and pancreatic lipase activities. *J. Agric. Food Chem.* **2011**, *59*, 9506−9511.
(25) Li, Y. Q.; Zhou, F. C.; Gao, F.; Bian, J. S.; Shan, F.; Zhao, C. Study on the interaction between 3 flavonoid compounds and α-amylase by fluorescence spectroscopy. *J. Food Sci.* **2009**, *74*, C199−C203.
(26) Eftink, Maurice R.; Camillo, A. Ghiron Fluorescence Quenching Studies with Proteins. *Anal. Biochem.* **1981**, *114*, 199−227.
(27) Unneberg, P.; Merelo, J. J.; Chacón, P.; Morán, F. SOMCD: method for evaluating protein secondary structure from UV circular dichroism spectra. *Proteins: Struct., Funct., Genet.* **2001**, *42*, 460−470.
(28) Li, Y. Q.; Zhou, F. C.; Gao, F.; Bian, J. S.; Shan, F. Comparative evaluation of quercetin, isoquercetin and rutin as inhibitors of α-glucosidase. *J. Agric. Food Chem.* **2009**, *57*, 11463−11468.
(29) Hawe, A.; Sutter, M.; Jiskoot, W. Extrinsic fluorescent dyes as tools for protein characterization. *Pharm. Res.* **2008**, *25*, 1487−1499.
(30) Park, J. H.; Ko, S.; Park, Hw. Toward the Virtual Screening of α-Glucosidase Inhibitors with the Homology-Modeled Protein Structure. *Bull. Korean Chem. Soc.* **2008**, *29*, 921−927.
(31) Park, H.; Hwang, K. Y.; Oh, K. H.; Kim, Y. H.; Lee, J. Y.; Kim, K. Discovery of novel α-glucosidase inhibitors based on the virtual screening with the homology-modeled protein structure. *Bioorg. Med. Chem.* **2008**, *16*, 284−292.
(32) Yoshimizu, M.; Tajima, Y.; Matsuzawa, F.; Aikawa, S.-I.; Iwamoto, K.; Kobayashi, T.; Edmunds, T.; Fujishima, K.; Tsuji, D.; Itoh, K.; Ikekita, M.; Kawashima, I.; Sugawara, K.; Ohyanagi, N.; Suzuki, T.; Togawa, T.; Ohno, K.; Sakuraba, H. Binding parameters and thermodynamics of the interaction of imino sugars with a recombinant human acid α-glucosidase (alglucosidase alfa): insight into the complex formation mechanism. *Clin. Chim. Acta* **2008**, *391*, 68−73.
(33) Chiba, S. Molecular mechanism in α-glucosidase and Glucoamylase. *Biotechnol., Biochem.* **1997**, *61*, 1233−1239.
(34) Jiang, X. Y.; Li, W. X.; Cao, H. Study of the Interaction between Trans-resveratrol and BSA by the Multi-spectroscopic Method. *J. Solution Chem.* **2008**, *37*, 1609−1623.
(35) Li, J.; Ren, C.; Zhang, Y.; Liu, X.; Yao, X.; Hu, Z. Spectroscopic studies on binding of Puerarin to human serum albumin. *J. Mol. Struct.* **2008**, *885*, 64−69.
(36) Shang, Q.; Xiang, J.-F.; Tang, Y.-L. Screening α-glucosidase inhibitors from mulberry extracts via DOSY and relaxation-edited NNR. *Talanta* **2012**, *97*, 362−367.
(37) Liu, X.-H.; Xi, P.-X.; Chen, F.-J.; Xu, Z.-H.; Zeng, Z.-Z. Spectroscopic studies on binding of 1-phenyl-3-(coumarin-6-yl)-sulfonylurea to bovine serum albumin. *J. Photochem. Photobiol., B* **2008**, *92*, 98−102.
(38) Du, Z.; Liu, R.; Shao, W.; Mao, X.; Ma, L.; Gu, L.; Huang, Z.; Chan, A. S. C. α-Glucosidase inhibition of natural curcuminoids and curcumin analogs. *Eur. J. Med. Chem.* **2006**, *41*, 213−218.
(39) Wang, Y.; Ma, L.; Li, Z.; Du, Z.; Liu, Z.; Qin, J.; Wang, X.; Huang, Z.; Gu, L.; Chen, A. S. C. Synergetic inhibition of metal ions and genistein on α-glucosidase. *FEBS Lett.* **2004**, *576*, 46−50.
(40) Tsujimoto, Y.; Tanaka, H.; Takemura, R.; Yokogawa, T.; Shimonaka, A.; Matsui, H.; Kashiwabara, S.; Watanabe, K.; Suzuki, Y. Molecular Determinants of Substrate Recognition in Thermostable α-glucosidases Belonging to Glycoside Hydrolase Family 13. *J. Biochem.* **2007**, *142*, 87−93.
(41) Bharatham, K.; Bharatham, N.; Park, K. H.; Lee, K. W. Binding mode analyses and pharmacophore model development for sulfonamide chalcone derivatives, a new class of α-glucosidase inhibitors. *J. Mol. Graphics Modell.* **2008**, *26*, 1202−1212.
(42) Hansawasdi, C.; Kawabata, J. α-Glucosidase inhibitory effect of mulberry (Morus alba) leaves on Caco-2. *Fitoterapia* **2006**, *77*, 568−573.
(43) Francis, F. J.; Markakis, P. C. Food colorants: anthocyanins. *Crit. Rev. Food Sci. Nutr.* **1989**, *28*, 273−314.
(44) Mei, M.; Ruan, J.-Q.; Wu, W.-J.; Zhou, R.-N.; Lei, J. P.-C.; Zhao, H.-Y.; Yan, R.; Wang, Y.-T. In vitro pharmacokinetic characterization of mulberroside A, the main polyhydroxylated stilbene in mulberry (Morus alba L.), and its bacterial metabolite oxyresveratrol in traditional oral use. *J. Agric. Food Chem.* **2012**, *60*, 2299−2308.